

# An Upper Bound on the Critical Volume in a Class of Toric Sasaki-Einstein Manifolds

Maksymilian Manko<sup>1,2\*</sup>

<sup>1</sup>London Institute, Royal Institution of Great Britain, 21  
Albemarle Street, Mayfair, London, W1S 4BS, UK.

<sup>2</sup>Linacre College, University of Oxford, St.Cross Road, Oxford,  
OX1 3JA, UK.

[maksymilian.manko@linacre.ox.ac.uk](mailto:maksymilian.manko@linacre.ox.ac.uk);

## Abstract

We prove the existence of an upper bound on critical volume of a large class of toric Sasaki-Einstein manifolds with respect to the first Chern class of the resolutions of the Gorenstein singularities in the corresponding toric Calabi-Yau varieties. We examine the canonical metrics obtained by the Delzant construction on these varieties and characterise cases when the bound is attained. We comment on computational tools used in the investigation, in particular Neural Networks and the gradient saliency method.

**Keywords:** Sasakian Manifolds, Calabi-Yau Varieties, Toric Geometry, Machine Learning

# 1 Introduction

The problem of determining the critical volume of Sasakian manifolds, as part of the wider program of finding Calabi-Yau manifolds and varieties among the Kähler ones, was defined and thoroughly studied at the turn of the century [1–4]. Akin to it as well, it was motivated by the study of gauge- and string-theoretical concepts, in particular the early investigations of the AdS/CFT correspondence [2, 5–8]. There the *a-minimisation* problem concerned finding the central charge and chiral operators at a conformal fixed point of a class of superconformal field theories. It was soon noticed that for toric varieties this procedure is geometrically dual to the minimisation of the volume among the corresponding compact Sasakian bases of (real) Kähler cones with respect to the Reeb vector field realised as a Euclidian vector inside a certain polyhedral cone. This *Z-minimisation* is in turn equivalent to the Ricci-flatness condition and the Sasaki base being Einstein, which means its Ricci curvature 2-form is proportional to the metric.

More recently there have been renewed interest in the problem [8, 9], as to the relatively short list of explicitly known Sasaki-Einstein metrics another item was added - vast datasets of toric Calabi-Yau varieties corresponding to reflexive lattice polytopes in 2, 3 and 4 dimensions [10, 11] that possess the desired presentation as Kähler cones. With the advent of more effective computational tools it became possible to compute the critical volumes for large sets of Sasaki-Einstein manifolds and multiple new observations regarding them followed. In this paper we are primarily concerned with the following result, which we will call the main theorem.

**Theorem 1.** (Part of Conjecture 5.5 of [8]). The critical volume of a Sasaki-Einstein base of a Calabi-Yau cone constructed over a reflexive polytope is bounded from above by

$$\text{Vol}(b^*, Y) = \frac{1}{n^n} \int_V c_1(\tilde{X})^{n-1} \quad (1)$$

As will be elaborated on below, here  $Y$  is the Sasaki-Einstein manifold,  $b^*$  is the critical Reeb vector and  $c_1(\tilde{X})$  is the first Chern class of the resolution of the Gorenstein singularity in the Calabi-Yau cone  $X$ . While originally stated as observational fact for reflexive polytope-genic Calabi-Yau varieties in dimensions 2, 3, we will prove this result in fact holds for all toric varieties whose toric diagrams have non-empty interiors. We also examine the varieties whose bases' volumes, as also observed in [8], in fact saturate the upper bound. The paper is organised as follows: in the first section we introduce the necessary devices of Sasakian and toric geometry, as well as the full statement of the  $Z$ -minimisation problem. In the second section we present the proof of the main theorem as well as the characterisation of the varieties where the bound is attained and link their metrics to the canonical metrics obtained

via the Delzant construction. In the appendix we briefly comment on the computational aspects of the investigation after summarising the work.

## 2 Theoretical background

We start by introducing relevant concepts from differential and toric geometry and fixing the notation for all the objects involved.

### 2.1 Sasakian preliminaries

As mentioned in the introduction, Sasakian manifolds are a class of contact manifolds which give rise to Kähler varieties as real cones [12]. The elements of the contact structure are crucial for our construction and turn out to relate closely to this *transverse* Kähler geometry. Throughout this paper we denote the full cone by  $X$  with complex dimension  $n$ , and the Sasakian base by  $Y$ , whose real dimension is clearly  $2n - 1$ .

#### 2.1.1 Contact and transverse symplectic structures

For the manifold  $Y$  we define the contact structure as follows, adapted from [13].

**Definition 1.** The contact structure on a manifold  $Y$  is a field of one-forms  $\alpha$  called the *contact form field*, such that locally for each point  $p \in Y$  we have a splitting of the tangent space

$$T_p Y = \ker \alpha_p \oplus \ker d\alpha_p, \quad (2)$$

so that the restrictions  $d\alpha_p|_{\ker \alpha_p}$  and  $\alpha_p|_{\ker d\alpha_p}$  are non-degenerate. In particular,  $d\alpha$  defines the *transverse* symplectic form, which extends to one on the cone  $X$ . In case the contact form is global the pair  $(Y, \alpha)$  is referred to as the *contact manifold*.

Note that a given manifold can admit multiple (indeed infinitely many [14]) contact structures. The related concept central to this paper is the Reeb vector field.

**Definition 2.** For a given contact form  $\alpha$  on  $Y$  the Reeb vector field is the unique vector field  $\xi$  such that

$$\iota_\xi \alpha = 1 \quad (3)$$

and

$$\iota_\xi d\alpha = 0 \quad (4)$$

where  $\iota$  is the interior product.

Following [3], we use  $\xi$  for the abstract Reeb vector and reserve  $b$  for its numeric presentation in the toric context.

We are now in position to define the Sasakian structure. Note that for this (as for the Kähler structure) we require a choice of Riemannian metric  $g$ , in consequence a *metric contact* structure [14]. However, it is always possible on a smooth manifold to introduce one and this choice will not bear on further discourse.

**Definition 3.** Let  $(Y, g_Y, \alpha)$  be a metric contact manifold. Define  $X \cong Y \times \mathbb{R}_+$  to be a cone over it, with the real coordinate  $r$  and the metric

$$g_X = dr^2 + r^2 g_Y. \quad (5)$$

$(Y, g_Y, \alpha)$  is a Sasakian manifold if and only if  $(X, g_X, d\alpha)$  ( $d\alpha$  naturally extended to the cone) is a Kähler manifold, i. e. there exists an integrable complex structure  $J$  such that for any vector fields  $x, y$  on  $X$

$$g_X(Jx, y) = d\alpha(x, y). \quad (6)$$

From this form the base can be retrieved as

$$Y = X|_{r=1}. \quad (7)$$

Importantly, there is a connection between the Reeb vector on the base  $Y$  and complex structure on the cone  $X$ , in terms of the Euler vector field associated to the cone coordinate  $r\partial/\partial r$

$$\xi = J \left( r \frac{\partial}{\partial r} \right). \quad (8)$$

A useful concept is the one of Kähler potential, which allows to easily obtain Kähler forms from certain scalar functions by utilizing the Dolbeault operators  $\partial, \bar{\partial}$ .

**Definition 4.** Let  $z_1, \dots, z_n, \bar{z}_1, \dots, \bar{z}_n$  be a patch of complex coordinates on a Kähler manifold  $X$ . If  $\varphi(z_i, \bar{z}_i)$  is *strictly plurisubharmonic*, i.e. its Hessian matrix at a point  $p$ ,  $(\frac{\varphi}{\partial z_i \partial \bar{z}_j})|_p$  is positive-definite for all vectors in  $T_p X$ , then

$$\frac{i}{2} \partial \bar{\partial} \varphi = \omega \quad (9)$$

where  $\omega$  is a Kähler form.

As an important example [1], the Kähler potential corresponding to a cone over a Sasakian manifold is

$$F = r^2. \quad (10)$$

We will use the Kähler potential in further sections in the discussion of its Legendre transform, the *symplectic potential*.

### 2.1.2 The Reeb foliation and regularity

By the first condition of def. 2, the Reeb vector field  $\xi$  is nowhere zero and so defines the *Reeb foliation* [1]. The properties of the orbits of this foliation induce the following classification of Sasakian metrics [3].

- If all the orbits close,  $\xi$  induces a circle action on  $Y$ . If this action is moreover free,  $Y$  fibrates into an  $S^1$  bundle  $\pi_\xi : Y \rightarrow V$  over a Kähler manifold  $V$ , which inherits the metric  $g_V$  from the transverse (cone) on  $g_X$  by push-down, together with the corresponding Kähler form  $\omega_V$ . In this case the Sasakian manifold is called *regular*.
- If more generally the  $U(1)$  action of  $\xi$  is only locally free and its orbits close the manifold is called *quasi-regular*. Then the fibration  $\pi_\xi : Y \rightarrow V$  is to a Kähler orbifold. Also locally at a given point  $p \in Y$ , the isotropy group is a non-trivial  $\Gamma_p \subset U(1)$ , which means  $\Gamma_p \cong \mathbb{Z}_m$  for some integer  $m$ . Then the length of the orbit is  $1/m$  of the generic (regular-esque) orbit.
- Finally if the orbits of  $\xi$  do not close, the Sasakian manifold is *irregular*. The orbits are then diffeomorphic to the real line.

As we will see later, critical Sasaki-Einstein metrics can belong to either of the classes.

Crucial to our main result is the following fact [15], [14].

**Theorem 2.** Any Sasakian manifold admits at least one quasi-regular metric.

Another important consequence of this characterisation is related to the Ricci curvature. The following relation holds (as a result of Einstein condition for  $Y$ )

$$\text{Ricc}(g_X) = \text{Ricc}(g_Y) - (2n - 2)g_Y = \text{Ricc}(g_T) - 2ng_T \quad (11)$$

where  $g_T$  is the transverse metric - the metric on  $X$  derived from  $Y$  contact structure. In particular if  $\rho$ ,  $\rho_T$  are the Ricci 2-forms of  $X$  and transverse respectively, and  $\omega_T$  is the transverse Kähler form, we have

$$\rho = \rho_T - 2n\omega_T. \quad (12)$$

Fit to our purposes, consider the case where  $X$  in fact admits a Calabi-Yau metric. Then there exists a  $n$ -holomorphic volume form, which on a generic complex coordinate patch  $(z_1, \dots, z_n)$  trivialises as

$$\Omega = dz_1 \wedge \dots \wedge dz_n. \quad (13)$$

Then it is known that if we consider the contraction  $\|\Omega\|_{g_X}^2 = 1/n! \Omega - \bar{\Omega}$ , the Ricci form can be obtained in the potential-like fashion as

$$\rho = i\partial\bar{\partial}\log\|\Omega\|_{g_X}^2. \quad (14)$$

Now if  $Y$  is quasi-regular, the transverse forms correspond to the pushdown forms (in the orbifold sense)  $\omega_V, \rho_V$ . Moreover, eq. (14), now pushed-down, is  $i\partial\bar{\partial}$ -exact on  $V$  [3]. we obtain an equation in the orbifold topology

$$[\rho_V] - 2n[\omega_T] \in H_{orb}^2(V; \mathbb{R}) \quad (15)$$

so that the Ricci and Kähler form belong to the same class. Since in general  $c_1(V) = [\rho/2\pi]$ , we see that  $V$  is in fact Fano, and crucially for the further discussion, the Kähler form belongs to the first Chern class. This will provide us with one of the ways to compute volume of  $Y$  in the quasi-regular case. Over the course of this paper we will drop the indices referring to the various objects without confusion, and similarly we will not distinguish between relevant definitions on manifolds and orbifolds unless relevant to the discussion.

## 2.2 Toric preliminaries

Among complex varieties the *toric* are ones admitting an effective torus action  $\mathbb{T}^n$  of rank equal to their dimension [1, 16]. This class of varieties is particularly interesting for its well-behavedness, stemming largely from the fact that computation of numerous quantities can be reduced to combinatorics of lattice polytopes, which is among the reasons motivating this study. Throughout this section we concentrate on how certain properties of Kähler cones and their Sasakian bases can be conveyed this way.

### 2.2.1 Torus actions and moment maps

The main technical tool for this task is the *moment map*, which establishes the relation between the original cone and a convex polyhedral cone we denote  $\mathcal{C}^*$  after [3].

Let us describe the cone using a set of toric coordinates  $\phi_1, \dots, \phi_n$ , such that  $\phi_i + 2\pi \sim \phi_i$  for all  $1 \leq i \leq n$ . Let also  $\mathfrak{t}_n$  be the Lie algebra corresponding to the torus  $\mathbb{T}^n$  and  $\mathfrak{t}_n^*$  its dual. We then have the following definition.

**Definition 5.** With the above notation, the moment map  $\mu : X \rightarrow \mathfrak{t}_n^*$  for a  $y \in \mathfrak{t}_n$  and dual pairing  $(\cdot, \cdot)$  is

$$(Y, \mu) = \frac{1}{2}r^2\alpha(Y). \quad (16)$$

It was shown in [17] that the image of  $X$  under  $\mu$  is a *rational polyhedral cone*  $\mathcal{C}^* \subset \mathfrak{t}_n^*$ . If we represent the abstract Reeb vector field  $\xi$  as  $b \in \text{Int } \mathfrak{t}_n^*$ .

The image of the base  $Y = X|_{r=1}$ , is then

$$2\langle b, y \rangle = 1 \quad (17)$$

where  $y \in \mathcal{C}^*$  and  $\langle \cdot, \cdot \rangle$  is the standard scalar product. Then we have the following result [3].

**Theorem 3.** The intersection

$$\Delta(b) = \mathcal{C}^* \cap 2\langle b, y \rangle = 1 \quad (18)$$

is a compact convex polytope if and only if  $b$  lies in the interior of the cone  $\mathcal{C} \subset \mathfrak{t}_n$ , dual to  $\mathcal{C}^*$  in the sense of Lie algebras.

Importantly, we can present this cone duality geometrically. In particular, the cone  $\mathcal{C}^*$  can be expressed as a set generated by the rays

$$\mathcal{C}^* = \left\{ \sum_a \lambda_a v_a \mid \lambda_a \geq 0 \right\} \quad (19)$$

which consists of real-valued vectors, and then the dual cone is the set

$$\mathcal{C} = \{ \nu \in \mathbb{R}^n \mid \langle v_a, \nu \rangle \geq 0 \} \quad (20)$$

which by Farkas's theorem is also a rational polyhedral cone [4]. This point will be crucial for the main proof.

### 2.2.2 Symplectic and Kähler potentials

There is an important link between the symplectic and toric aspects of the varieties, established by the use of symplectic potential. Let us introduce symplectic coordinates, related to the previous toric ones  $\phi_i$  by

$$y_i = \mu \left( \frac{\partial}{\partial \phi_i} \right) \quad (21)$$

This renders the Kähler form

$$\omega = \sum_{i=1}^n dy_i \wedge d\phi_i \quad (22)$$

and the metric

$$ds^2 = G_{ij} dy_i dy_j + G^{ij} d\phi_i d\phi_j \quad (23)$$

where Einstein convention was employed,  $G_{ij}$ ,  $G^{ij}$  are a matrix and its inverse respectively. The scalar  $G$  is then called the symplectic potential with

$$G_{ij} = \frac{\partial^2 G}{\partial y_i \partial y_j}. \quad (24)$$

By the Kähler compatibility condition, the complex structure trivialises to

$$J = \begin{bmatrix} 0 & -G^{ij} \\ G_{ij} & 0 \end{bmatrix} \quad (25)$$

From the observation

$$r \frac{\partial}{\partial r} = 2y_i \frac{\partial}{\partial y_i} \quad (26)$$

one can deduce that

$$b_i = 2G_{ij}y_j \quad (27)$$

assuming Einstein convention. Finally, as mentioned previously, the symplectic potential is related to the Kähler potential  $F$  by the Legendre transform. Let  $z_i = x_i + i\phi$  be log-complex coordinates on the Kähler cone  $X$ , such that  $z_i = \log w_i$  and  $w_i$  are standard coordinates on the punctured complex space  $\mathbb{C}^n/\{0\}$ . In these terms, by def. (4), the metric would take form

$$ds^2 = F_{i\bar{j}} dx_i d\bar{x}_j + F^{i\bar{j}} d\phi_i d\bar{\phi}_j \quad (28)$$

with

$$F_{i\bar{j}} = \frac{\partial^2 F}{\partial x_i \partial \bar{x}_j}. \quad (29)$$

It was shown in [4] that the two potentials fulfill

$$F(x) = \left( y_i \frac{\partial G}{\partial y_i} - G \right) \left( y = \frac{\partial F}{\partial x} \right) \quad (30)$$

with the moment map being then clearly

$$\mu = \frac{\partial F}{\partial x}. \quad (31)$$

### 2.2.3 The Monge-Ampère equation

In this short section we briefly recount the Monge-Ampère equation for the Calabi-Yau condition, as derived in [4], in order to introduce two results important for our discourse.

Firstly, recall from eq. (14) that the Ricci 2-form can be obtained in a potential-like fashion. Indeed the Kähler potential can also be used for this purpose, in particular its matrix

$$\rho = -i\partial\bar{\partial} \log \det(F_{i\bar{j}}). \quad (32)$$

This is in general flat if the differentiated quantity is linear, or

$$\log \det(F_{ij}) = -2x_i \gamma_i + c \quad (33)$$

for  $y_i, c$  all constant. Reverting the Legendre transform yields the Monge-Ampère equation in symplectic coordinates

$$\det(G_{ij}) = \exp \left( 2\gamma_i \frac{\partial G}{\partial y_i} - c \right). \quad (34)$$

Now, the discussion in [4] shows that for a Gorenstein singularity, our case of interest, eq. (34) is only possible if

$$-n = \langle y, b \rangle. \quad (35)$$

This is solved by

$$b_n = n \quad (36)$$

and  $\gamma = (0, \dots, -1)$  so that

$$\log \det(F_{ij}) = 2x_n + c. \quad (37)$$

Both these conditions will turn out helpful in discussion of the saturation of our sought upper bound for the volume.

## 2.2.4 Toric diagrams and Hilbert series

There has been a considerable interest recently towards the study of varieties arising from lattice polytopes, fuelled by the advent of the complete datasets of these objects, most notably the one due to Kreuzer and Skarke amassing beyond half a billion of reflexive polytopes [8, 10], that can be probed with computational methods.

The construction of Kähler cones in question, although usually considered in the algebro-geometric context, is coherent with the previous discussion. In particular, the *a priori* choice of polytope allows to fix certain properties of the variety and related quantities. Denote by  $\Delta_{n-1}$  a convex polytope of dimension  $n-1$  (recall  $n$  referred to the dimension of the Kähler cone  $X$ ) with vertices  $w_1, \dots, w_d$ . We construct the polyhedral cone  $\mathcal{C}^*$  from theorem 3 by attaching an  $n$ th coordinate of value 1 to each of the vertices

$$v_a = (w_a, 1), \quad 1 \leq a \leq d. \quad (38)$$

This also implies that the cone  $X$  is constructed over a *Gorenstein singularity* [4, 8]. Treating  $v_a$  as generating rays, we allow the cone to diverge to infinity, as shown in fig. 1. Immediately by the inverse of the moment map we retrieve the Sasaki base as  $Y = \mu^{-1}(\Delta)$ , as well as the correct non-compact asymptotics. Let  $v_a$  denote the inward vectors normal to the facets (following the indexing

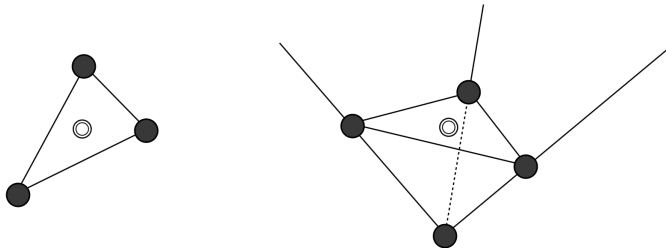


**Fig. 1** The 2-dimensional reflexive polytope of the 0th del Pezzo surface (a cone over a flat projective space) and its corresponding polyhedral cone. The white bullet indicates the 2D lattice origin

as above). Immediately also

$$v_a^n = 1 \quad 1 \leq a \leq d \tag{39}$$

We will refer to the behaviour in eqs. (36), (38) and (39) collectively as the *co-planarity condition*, which will be crucial for the main proof.

Instead of considering the moment map, the cone is obtainable directly via toric methods as presented in [8, 9, 16]. Consider the normal vectors of eq. (39) as n-tuplewise generating affine cones, one for each facet. This is called the *face fan* of a toric variety. By devising pairwise rational transition functions for these cones, one obtains a non-compact toric variety, the one corresponding to the othe del Pezzo surface dP0 is shown in fig. 2. The polytope, now dubbed

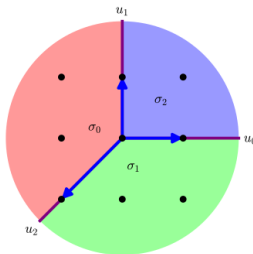


**Fig. 2** Face fan corresponding to the 0th del Pezzo surface

*toric diagram* provides us then with additional information that will allow us to calculate the volume of the Sasaki base. Formally, it encodes the graded pieces (components of the variety generated by polynomials of a given (multi-)degree) of  $X$  in a formal series

$$H(t_1, \dots, t_n, X) = \sum_{i=0}^{\infty} (\dim_i X) t_1^{i_1} \dots t_n^{i_n} \tag{40}$$

where  $\mathbf{i}$  is a multi-index in the dimension of the variety.

For the toric setting, there is a polytope-combinatorial formula rendering the series, as shown in [8]. A necessary step to use it (and a major computational obstacle as reported later) is to perform fine, regular and stellar (FRS) triangulation of  $\Delta$ , which is one resulting in a set of simplexes such that there is an edge connecting any two points on the surface or in the interior of the polytope. Let  $\nu_{ij}$  be the associated (outward) normal vectors to the facets of the simplexes, where  $1 \leq i \leq r$ ,  $1 \leq j \leq n$ , running over the set of simplexes and lists of their facets respectively, so that the multi-exponent gives the product of formal variables raised to the powers of vector components. Then

$$H(t_1, \dots, t_n, X) = \sum_{i=1}^d \prod_{j=1}^n (1 - t^{\nu_{ij}})^{-1}. \quad (41)$$

The latter form is of particular practical use as all the involved quantities are readily (albeit not rapidly) available using **Sage**.

### 2.2.5 Reflexive polytopes

One class of toric diagrams that has received increased attention recently is that of reflexive polytopes. This particular type allows to construct toric fans that are Gorenstein singularities which admit crepant resolutions (see [16] def. 8). *Reflexivity* is defined with respect to the *polar dual*.

**Definition 6.** For a lattice polytope  $\Delta$ , its polar dual is defined as

$$\Delta^\circ = \{w \in \mathbb{R}^n \mid \langle w, v \rangle \geq -1, \forall v \in \Delta\}. \quad (42)$$

Then  $\Delta$  is reflexive if and only if  $\Delta^\circ$  is also a lattice polytope, and since  $(\Delta^\circ)^\circ = \Delta$ , the dual is reflexive too. In fact, there is one particularly handy identifying property of these, as outlined in [16].

**Theorem 4.** A polytope  $\Delta$  is reflexive if and only if its sole internal point is the origin of the lattice.

We will exploit this in the main proof.

## 2.3 The volume function of $Y$

As outlined in the introduction, the centrepiece of the  $Z$ -minimisation problem is the normalised volume of the Sasakian base  $Y$ . In particular, as shown in [1] we have the following theorem.

**Theorem 5.** The normalised volume function  $\text{Vol}$  of  $Y$

$$\text{Vol}(Y, b) = \frac{\text{vol}(Y, b)}{\text{vol}(S^{2n-1})} \quad (43)$$

is a convex continuous function possessing a global minimum, of the trivialisation of the Reeb vector in  $\mathcal{C}$ ,  $b$ . The function  $\text{vol}$  refers to the volume with respect to the Sasakian metric on  $Y$ . We indicate this critical vector by  $b^*$ .

Although there are several methods to obtain the volume function [2], [4], including directly from the original physical  $a$ -function [4, 5], the most viable for the present case is the one using the Hilbert series [8, 9, 16], (also coinciding in this context with the *index-character* of [3]). The normalised volume function is retrieved from the following limit.

$$\text{Vol}(Y, b) = \lim_{\epsilon \rightarrow 0} \epsilon^n H(\exp(-\epsilon b)) \quad (44)$$

where the Reeb vector  $b$  takes the role of the list of the formal parameters. The meaning of this limit is to retrieve the leading term of the series (which for toric setting is necessarily finite [8]), and is always a rational function in the components of  $b$ . Existence of (44) justifies this computational approach, as it can be purely algorithmically implemented in standard symbolic packages, such as `Mathematica`, `Sage` or `SymPy`. For the example of the 0th del Pezzo surface  $dP_0$ , whose toric diagram is presented in fig. 1, the volume function is

$$\text{Vol}(b, dP_0) = \frac{9}{(b_1 - 2b_2 - b_3)(2b_1 - b_2 + b_3)(b_1 + b_2 - b_3)}, \quad (45)$$

which is minimised by the vector  $b^* = (0, 0, 3)$  so that  $\text{Vol}(b, dP) = \frac{1}{3}$ . In general, however, the critical vector  $b^*$  is composed of *algebraic* numbers as shown in [1]. Indeed there it is shown that

**Proposition 1.** The critical vector  $b^*$  is rational if and only if the corresponding Sasakian structure is quasi-regular (or regular).

As will be observed in further sections, the generic  $b^*$  tends to be algebraic, and so the corresponding structure irregular.

### 2.3.1 Volume function of quasi-regular Sasakian manifolds

In this section we address the notion that the volume for a quasi-regular Sasakian structure is in fact a topological quantity [1, 3]. This is a key point to our main proof, as we now outline.

Recall the main theorem 1 refers to a resolution of the Gorenstein singularity of  $X$  and its first Chern class. We wish to relate it to the volume of  $Y$ . In

particular we expect the volume to be independent of the resolution map,

$$\Pi : \tilde{X} \rightarrow X. \tag{46}$$

It was shown to be indeed so in [3], up to orbifold singularities, which is sufficient for our purposes. Moreover, it is possible to do so using the leaf space of the Reeb foliation, the Kähler orbifold  $V$ . Now,  $V$  exists as such only for (quasi-) regular structures, but at least one of these is always present for any Sasakian manifold per theorem 2. As explained in section 2.1.2, in the (quasi-)regular case, the Reeb foliation is in fact a fibration over a Kähler (orbi-)manifold  $V$ , with the real projection

$$\pi_\xi : Y \rightarrow V. \tag{47}$$

If  $\pi_\xi$  is viewed as a holomorphic function (away from the origin), there is a corresponding complex (orbi) bundle  $\mathcal{L}$ . If  $W$  is the total space of this bundle then the quotient  $W/V \cong X$  furnishes the desired resolution. For the sake of brevity, and by combining theorem 2 and eq. 51, we will often abuse notation by using  $c_1(V)$  even if  $c_1(\tilde{X})$  is more appropriate.

There is a correspondence between the first Chern classes of  $V$  and  $\mathcal{L}$  in the orbifold cohomology

$$c_1(\mathcal{L}) = \frac{c_1(V)}{\beta} \in H_{orb}^2(V; \mathbb{Z}). \tag{48}$$

We defined the cohomology to be integer, but as explained in the remark 1, both classes could be multiplied by the same algebraic constant. Let additionally

$$\pi_r : X \rightarrow Y \tag{49}$$

be the projection along the axis of the cone, and

$$q : W \rightarrow X \tag{50}$$

be the quotient map described above. Observe that by construction we have that a structure  $\xi$  is quasi-regular if and only if the diagram

$$\begin{array}{ccc} W & \xrightarrow{\Pi} & X \\ \pi'_\xi \uparrow & & \downarrow \pi_r \\ V & \xleftarrow{\pi_\xi} & Y \end{array} \tag{51}$$

where  $\pi'_\xi$  is the blow-up of  $V$  associated to the complex line bundle  $\mathcal{L}$ , is well-defined (in the sense that all the maps are well-defined). The identity map here refers to the natural association on the grounds that the result is independent on the choice of resolution. Now, as a consequence of the Duistermaat-Heckman

formula [18] it was shown in [3] that the volume of the quasi-regular  $Y$  is given by

$$\text{Vol}(b) = \frac{1}{b^n} \int_V c_1(\mathcal{L}^*)^{n-1} \quad (52)$$

where  $c_1(\mathcal{L}^*) = -c_1(\mathcal{L})$ .

On the other hand recall from eq. (12) that the Kähler class corresponds to the first Chern class. By the standard result the Kähler form allows to compute the volume of a compact manifold (note the  $n-1$  dimension due to the pushdown), which is thus proportional to the first Chern number (the class integrated over its host space)  $c_1$ .

$$\text{Vol}(b) = \int_V \frac{\omega_V^{n-1}}{(n-1)!} = \frac{\pi^{n-1}}{n^{n-1}(n-1)!} \int_V c_1(V)^{n-1}. \quad (53)$$

Since in our theorem 5 we compare the volume to the one of the round sphere  $\text{vol}(S^{2n-1}) = \frac{2\pi^n}{(n-1)!}$ , and noting that  $2\pi\beta/n$  is the fiber length for the foliation [3], we obtain

$$\text{Vol}(b) = \frac{\beta}{n^n} \int_V c_1(V)^{n-1}. \quad (54)$$

It is clear that for eqs. (52) and (54) to coincide, we need to set

$$\beta = \frac{n}{b}. \quad (55)$$

For our running example, the 0th del Pezzo surface,  $b^* = (0, 0, 3)$ , so that  $\beta = 1$ . On the other hand its  $c_1 = 9$ , so that the corresponding result of eq. (54) coincides with the original one of eq. (45).

**Remark 1.** The comparison of eqs. (52), (54), (55) might appear artificial. Indeed, for computational purposes one needs to be more careful with choosing the normalisation for objects that derive from the Reeb vector action, including topological numbers of  $\mathcal{L}$  and  $V$  as well as  $\beta$  to avoid invalidities such as irrational Chern numbers. Here we fix it by demanding (55) be true, and choosing normalisations for (52) and (54) to coincide with it, in order to adhere to the original conjecture of [8]. Fortunately, our proof relies chiefly on the reciprocal dependence of the volume and  $\beta$  on the norm of the Reeb vector, which turns out to be sufficient, as long as the normalisation is controlled.

### 2.3.2 The Delzant canonical structure

Before introducing the conditions for Ricci-flatness of the metric on  $X$ , we introduce the *canonical structure*, due to Delzant, as outlined in [3, 19]. It utilises *symplectic reduction* and has the advantage of being easily obtainable from the toric diagram. Consider the linear map

$$A : \mathbb{R}^d \rightarrow \mathbb{R}^n$$

$$e_a \mapsto v_a \quad (56)$$

where  $e_a$  form the standard basis for  $\mathbb{R}^d$  and  $v_a$  are the normal vectors of the facets on the toric diagram. Denote additionally by  $\Lambda$  the span of the normals  $v_a$  over  $\mathbb{Z}$ , which should give a lattice of maximal rank. Then there is an induced map of tori

$$\mathbb{T}^d \cong \mathbb{R}^d / 2\pi\mathbb{Z}^d \rightarrow \mathbb{R}^n / 2\pi\Lambda. \quad (57)$$

Its kernel then fulfills  $\ker A \cong \mathbb{T}^{d-n} \times \Gamma$ , for a finite abelian group  $\Gamma$ . Thus  $X$  is a symplectic quotient

$$X = \mathbb{C}^d // \ker A. \quad (58)$$

As mentioned above its properties are easily obtained from the toric diagram. Firstly, the canonical symplectic potential (which allows to find metric and the Kähler form) in terms of symplectic coordinates is given by

$$G^{can}(y) = \frac{1}{2} \sum_a \langle y, v_a \rangle \log \langle y, v_a \rangle. \quad (59)$$

Using eq. (27) the canonical Reeb vector becomes

$$b^{can} = \sum_a v_a \quad (60)$$

which forces  $b_n = d$ , the number of facets of the polytope. For our running example, the 0th del Pezzo surface this gives  $b^{can} = (0, 0, 3)$  as its toric diagram is a triangle. In general, a symplectic potential for a Reeb vector  $b$  can be obtained from the canonical one as follows. Define

$$G_b(y) = \frac{1}{2} \langle b, y \rangle \log \langle b, y \rangle - \frac{1}{2} \sum_a \langle b^{can}, y \rangle \log \left( \sum_a \langle b^{can}, y \rangle \right). \quad (61)$$

Then, as a consequence of the fact that the moduli space of symplectic potential splits as  $\text{Int } \mathcal{C}^* \times \mathcal{H}(1)$ , where the polyhedral cone part controls the Reeb vector and  $\mathcal{H}(1)$  is the space of holomorphic homogenous degree 1 functions on  $X$ , we obtain

$$G(b) = G^{can} + G_b + g \quad (62)$$

with some  $g \in \mathcal{H}(1)$ . In particular by (24), two symplectic potential matrices  $G_{ij}, G'_{ij}$  are in fact the same if

$$G - G' = g = \lambda_i y_i + t \quad (63)$$

with  $\lambda_i, t$  all constant. One handy corollary of (62) is that

$$2y_i \frac{\partial}{\partial y_j} \frac{\partial}{\partial y_i} G_b = b_i - b_i^{can}. \quad (64)$$

This will be particularly useful for observations regarding when the upper bound for the metric is in fact saturated.

It is worthwhile to find the explicit form of the Kähler potential for the canonical structure. As it will be shown, it in fact has a general form as a product of exponential functions, in terms of  $b^{can}$

$$F^{can}(x) = N \exp\left(\frac{2x_1}{b_1^{can}}\right) \dots \exp\left(\frac{2x_n}{b_n^{can}}\right) \quad (65)$$

where  $N$  is some normalising constant we will fix.

Consider firstly the canonical symplectic potential of eq. (59). To perform the Legendre transform as in (4), we begin by considering the first derivatives of  $G^{can}$

$$y_i \frac{G^{can}}{\partial y_i} = \frac{1}{2} \sum_a (y_i + y_i \log \langle y, v_a \rangle) v_a^i \quad (66)$$

where  $v_a^i$  is the  $i$ th component of the corresponding normal. If we now take the sum over  $i$  as well we see that

$$\sum_i y_i \frac{G^{can}}{\partial y_i} = \frac{1}{2} \sum_i \sum_a (y_i + y_i \log \langle y, v_a \rangle) v_a^i = \frac{1}{2} \langle y, b^{can} \rangle + G^{can}. \quad (67)$$

Thus when this is substituted to (4), it yields

$$F^{can} = \left(\frac{1}{2} \langle y, b^{can} \rangle + G^{can} - G^{can}\right) = \frac{1}{2} \langle y, b^{can} \rangle. \quad (68)$$

where we distinguish between  $F$  - a function of  $y$  and  $F(x)$  - one fully transformed into  $x$ -coordinates. This gives a separable PDE

$$F^{can}(x) = \frac{1}{2} \sum_i b_i^{can} \frac{\partial F}{\partial x_i}, \quad (69)$$

whose solution is indeed (65) with  $N = 1$ . This also makes sense bearing in mind the  $x_i$  were obtained from log-complex coordinates, so in that context the exponential is neutralised and yields linear expressions of coordinates.

Finally recall eq. (32) and note that the canonical metrics seldom are Ricci flat, which we show is nevertheless the case for the structure saturating the bound. The 0th del Pezzo surface though does belong to this class (recall from eq. (45) the corresponding critical volume is rational) so its Kähler potential is

$$F(x) = \exp\left(\frac{2x_3}{3}\right) \quad (70)$$

with

$$\rho = -\partial\bar{\partial}(2x_3 - 3) = 0. \quad (71)$$

## 2.4 The Z-minimisation problem

With the entirety of our toolkit defined, we can proceed to the main problem which is identifying when the Kähler cone  $X$  admits a Calabi-Yau metric. Recall that a metric  $g$  is Einstein if it is proportional to the corresponding Ricci tensor  $\text{Ricc}_g$ ,  $\text{Ricc}_g = \lambda g$  for some constant  $\lambda$  (therefore all Calabi-Yau metrics are trivially Einstein). With reference to our problem we have the following theorem [3].

**Theorem 6.** The Kähler cone  $X$  is Ricci-flat (or Calabi-Yau) if and only if the volume of the Sasaki base is minimized with respect to the Reeb vector  $b$ . In fact if and only if the base is Sasaki-Einstein, with  $\lambda = 2(n - 1)$ .

Note also that since by the coplanarity condition  $b_n = n$ , the minimisation is practically performed in one variable less. Thus the problem of finding the Calabi-Yau metric on the cone (or Sasaki-Einstein metric on the base), in the toric setting reduces to an optimisation problem for convex rational functions, accessible entirely from polytope combinatorics.

While this is a truly neat result, the computational reality turns out less agreeable. Indeed multiple steps of the procedure, including the FRS triangulation and final optimisation, are exceptionally costly, with complexity ever increasing with dimension, effectively barring the half-billion Kreuzer-Skarke varieties from sound computational scrutiny. It is therefore advantageous to develop certain constraints on the volumes and parameter space, in terms of quantities available more easily, as attempted in [8].

## 3 The upper bound conjecture

In this section we prove the main theorem 1, as well as discuss a number of observations concerning this problem.

### 3.1 Proof of the main theorem

Recall firstly theorem 2, and the fact that any Sasakian manifold admits at least one (not necessarily critical) quasi-regular structure. Then the coplanarity conditions, force the corresponding Reeb vector to have  $b_n = n$ . This constrains the norm of the vector to be

$$b \geq n. \tag{72}$$

Further observe that as the consequence of theorem (4), for any reflexive polytope (of explicit dimension  $n - 1$ )  $\Delta_{n-1}$  we have the lattice origin  $0_n \in \Delta_{n-1}$ . Hence by the intersection condition eq. (3), as well as eq. (20) and co-planarity necessarily

$$\begin{aligned} b_0 &= (0, \dots, 0, n) \in \mathcal{C} \\ b_0 &= (0, \dots, 0, n) \in \mathcal{C}^* \end{aligned} \tag{73}$$

in the polyhedral cones defined previously. The two statements are easily checked against one another using the eq. (20) for the dual cone. This provides

a well-defined contact structure, because for a reflexive polytope the origin is always in the interior and never at the boundary of  $\mathcal{C}$ , avoiding any singularities.

Note that the structure corresponding to  $b_0$  is quasi-regular, since by substituting it into the toric volume function eq. (44) the result is always rational by construction.

From the condition (48), we see that  $\beta_0 = 1$ , and so eqs. (52) and (54) naturally coincide at

$$\text{Vol}(b_0, X) = \frac{1}{n^n} \int_V c_1(V)^{n-1}. \quad (74)$$

Therefore the structure  $b_0$  saturates the bound for any cone  $X$  build upon a reflexive polytope. Now we know from theorem 5 that the volume function is continuous and convex function of  $b$ , with a global minimum. Thus  $b_0$  may or may not be the critical volume. If it is not, the critical volume  $\text{Vol}(b^*, X)$  will be strictly smaller than  $\text{Vol}(b_0, X)$ , which was to be proved.

Note that the key property of the  $b_0$  Reeb vector is that it occurs in all polyhedral cones and their duals corresponding to reflexive polytopes. In fact by the same reasoning for any set of toric diagrams, if we are able to find some  $b'$  that appears in all interiors of dual cones, its structure will also constitute a bound. Additionally, a (possibly infinite) set of such Reeb vectors will be ordered by the norms of the vectors according to our normalisation (55), so that the "longest" vector gives the strongest bound. Thus, by the fact the  $b_0$ -bound is saturated in the 3-dimensional polytopes, and it happens to be the "shortest" possible Reeb vector, we can conclude this is the only point of the dual cones that belongs to them for the entire set. Going one step further, we can consider any toric diagram with non-empty interior and translate it within the lattice so that it contains the lattice origin (which is always allowed with diagrams defined up to  $\text{GL}(n, \mathbb{Z})$  action), then the result holds for such toric Kähler cone as well. There exist, however, toric diagrams, such as the one of the suspended pinch point (SPP) [4], which is a Gorenstein singularity, but the lattice origin is contained in the boundary of the diagram rather than the interior. The boundary of SPP is in fact singular, so the original argument is not applicable here. Nevertheless, by theorem 2, there is at least one quasi-regular structure admitted by the SPP. Moreover, as shown in [4], the normalised volume of SPP is in fact irrational (i.e. the structure is irregular), equal to  $\frac{4\sqrt{3}}{9}$ , and corresponds to an algebraic  $b^*$  so that the existing quasi-regular structure would give a higher volume and some analogous bound can be established.

**Remark 2.** Interestingly enough  $b_0$  is also a fixed point of polar duality of reflexive polytopes, which means it is preserved by mirror symmetry of toric varieties [16]. A natural question arises whether this condition for the bound is sustained in the non-toric context.

**Remark 3.** As explained in [1],  $\mathcal{L}^\beta = \mathcal{K}$ , the canonical line bundle over  $V$ . Now if  $\beta = 1$  which is only possible for the  $b_0$  structure, in fact regardless of conditions of remark 1, then  $\mathcal{L}$ ,  $\mathcal{K}$  and  $X$  all coincide.

### 3.2 Characterisation of the $b_0$ structure

Having proved the upper bound as well as found the Reeb vector saturating it, we now proceed to make several observations regarding the structure  $b_0$ . We start with the following proposition

**Proposition 2.** If the volume of the given base  $Y$  saturates the bound i.e. its critical vector is  $b_0$ , then its canonical vector is  $b_0^{can} = (0, \dots, d)$ , where  $d$  is the number of facets of the corresponding polytope.

*Proof :* Firstly note that the canonical metric is in general not flat, in particular for  $d > n$  which violates co-planarity, so we cannot employ the mechanism of the main proof to make it coincide with the already critical  $b_0$ . Instead, consider eq. (64). We have

$$G_b = \frac{1}{2}ny_n \log(ny_n) - \frac{1}{2}\langle b^{can}, y \rangle \log\langle b^{can}, y \rangle. \quad (75)$$

For  $i < n$  this after derivation becomes

$$y_i \frac{\partial}{\partial y_j} \frac{\partial}{\partial y_i} G_b = y_j \frac{b_i^{can} b_j^{can}}{\langle b^{can}, y \rangle} = -b_i^{can}. \quad (76)$$

where Einstein summation convention was employed. Now, either  $b_i^{can} = 0$ , or we can divide both sides by it, in which case

$$\langle b^{can}, y \rangle = y_j b_j^{can} = -y_j b_j^{can} \quad (77)$$

which is a contradiction given that  $b_n = n$  and  $b_n^{can} = d$  are non-zero. Thus  $b_i = 0$  for  $i < n$ , which concludes the proof.  $\square$

As a corollary we immediately notice that if  $d = n$ , the canonical metric is flat. Also, from the Delzant symplectic reduction and eq. (57), we see that  $\ker A = \Gamma$ , so these cones are in fact abelian orbifolds of  $\mathbb{C}^n$ , which indeed agrees with the list for 3-dimensional abelian orbifolds in the appendix of [8]. With the observation in eq. (75), we can now compute the symplectic and Kähler potentials for  $b_0$ . While we can now easily deduce  $G_b$ , unfortunately non-linearly normals-dependent  $G^{can}$  indulges little insight (indeed computational expense for inverting  $G_{ij}$  makes the process unfeasible), so we have

$$\begin{aligned} G &= \frac{1}{2} \sum_a \langle y, v_a \rangle \log \langle y, v_a \rangle - \frac{1}{2} ny_n \log(ny_n) + \frac{1}{2} dy_n \log(dy_n) \\ &= \frac{1}{2} \sum_a \langle y, v_a \rangle \log \langle y, v_a \rangle - \frac{1}{2} (n \log(y_n) + y_n n \log n - d \log(y_n) - y_n d \log d). \end{aligned} \quad (78)$$

Recall, however, from eq. (63) that symplectic potentials differing by a linear function give the same metric. Hence we retain only the non-linear terms

$$G = \frac{1}{2} \sum_a \langle y, v_a \rangle \log \langle y, v_a \rangle + \frac{1}{2} (d - n) y_n \log y_n. \quad (79)$$

Luckily, the Kähler potential provides more intuition. Notice firstly that the Legendre transform is linear in the sense of adding symplectic potentials. In particular, the  $G_b$  component can be simply added to the  $G^{can}$  part already found in eq. (68) so that

$$F = F^{can} + F_b \quad (80)$$

where we again distinguish between  $F$  - a function of  $y$  and  $F(x)$  - one fully transformed into  $x$ -coordinates. The only derivative we need to consider is the one with respect to  $y_n$  (using the simplified  $G_b$  as above)

$$y_n \frac{\partial G_b}{\partial y_n} = \frac{1}{2} y_n (n - d) (\log y_n + 1). \quad (81)$$

We see that similarly as for the canonical case, the terms containing logarithm in (81) will be subtracted so that

$$F_b = \frac{1}{2} (n - d) y_n. \quad (82)$$

Moreover notice that for  $b^{can} = b_0^{can}$ ,  $F^{can}$  also simplifies considerably, so that

$$F = F^{can} + F_b = \frac{n}{2} y_n. \quad (83)$$

Before solving the PDE in the last step, let us pause for a couple of remarks. Firstly, if  $n = d$  we established that the canonical metric is flat and coincides with some abelian orbifold. Indeed we can see that then  $F = F^{can}$  and the two metrics are the same.

Secondly, notice that in general eq. (83) is independent of  $d$ , so that all cones with bases saturating the bound share the same metric. It was to be expected as we remarked previously that in this case the volume is a topological quantity, independent on the toric diagram, and since the Chern class coincides with the push-down Kähler class in the orbifold cohomology, it should not depend on the toric diagram either.

Let us now perform the final step of the Legendre transform. Obviously, in this case the only meaningful derivative is this with respect to  $y_n$ . Thus

$$F(x) = \frac{n}{2} \frac{\partial F(x)}{\partial x_n} \quad (84)$$

and eq. (65), reduces to

$$F(x) = \Phi(x_1, \dots, x_{n-1}) \exp\left(\frac{2x_n}{n}\right) \quad (85)$$

where  $\Phi(x_1, \dots, x_{n-1})$  is a scalar function independent of  $x_n$ . It is reasonable to choose

$$\Phi(x_1, \dots, x_{n-1}) = z_1 \bar{z}_1 + \dots + z_{n-1} \bar{z}_{n-1} \quad (86)$$

which is the Kähler potential of the flat metric on  $\mathbb{C}^{n-1}$ , in order to allow  $F(x)$  to indeed meaningfully fulfill def. 4. We see that

$$\begin{aligned} F_{ij} &= \frac{4}{n^2} \exp\left(\frac{2x_n}{n}\right) \quad \text{if } i = j = 4 \\ F_{ij} &= 1 \quad \text{if } i = j < 4 \\ F_{ij} &= 0 \quad \text{otherwise.} \end{aligned} \quad (87)$$

so that the metric is diagonal and non-trivial only in the dimension perpendicular to the polytope hyperplane.

Finally as a sanity check let us use eq. (32) to confirm Ricci-flatness. Obviously

$$\det(F_{ij}) = \frac{4}{n^2} \exp\left(\frac{2x_n}{n}\right) \quad (88)$$

logarithm of which gives indeed  $2x_n + c$  as in eq. (37) and so this metric is Ricci flat.

## 4 Summary and discussion

Summing up, over the course of this paper we proved the upper bound part of the conjecture 5.5 of [8] concerning an upper bound on the critical volume of Sasaki-Einstein manifolds, characterised these Calabi-Yau cones volumes of whose Sasaki-Einstein bases saturate it and finally discussed its links to the canonical Delzant metrics. While from the computational perspective this is a useful result, allowing to significantly constrain the space of possible critical volumes for toric varieties using the easily computable quantity  $c_1(V)$  it does not overcome the significant practical limitation in that the proof does not suggest a way to know *a priori* whether a particular cone saturates the bound or not, without the regular  $Z$ -minimisation procedure. Indeed for instance the proposition 2 lacks an 'only if' part, that would provide such a test, and the  $b_0$  structure exists on any toric Kähler cone, whose toric diagram has non-empty interior, without any regard to criticality. Moreover, it was shown in [1] that the volume function ultimately depends only on the vector  $b$ , and the analysis using neural networks presented in the appendix A strongly suggests that if any alternative avenue is available it lies beyond simple analysis of the toric diagrams and topology of related objects we presented. This, however, does

not rule out such possibility completely, in particular there has been significant effort in analysing the problem in more general algebro-geometric context such as in [15, 20] providing more insights. Indeed the second part of the conjecture 5.5 regarding the lower bound of the volume obtained from the Euler number of the cone remains open and could serve as motivation for further exploration.

**Acknowledgments.** I would like to thank Y-H. He for supervision and kind welcome at the London Institute and E. Hirst for helpful comments. The work was supported by the London Mathematical Society Undergraduate Research Bursary URB-2022-01.

**Declarations.**

**Conflict of interest statement.** The author declares no competing interests.

**Data accessibility statement.** The datasets generated during and/or analysed during the current study are available from the repository <https://github.com/lgrng/SasakiMLSaliency>.

**Open access.** This article is licensed under a Creative Commons Attribution 4.0 International License, which permits use, sharing, adaptation, distribution and reproduction in any medium or format, as long as you give appropriate credit to the original author(s) and the source, provide a link to the Creative Commons licence, and indicate if changes were made. The images or other third party material in this article are included in the article's Creative Commons licence, unless indicated otherwise in a credit line to the material. If material is not included in the article's Creative Commons licence and your intended use is not permitted by statutory regulation or exceeds the permitted use, you will need to obtain permission directly from the copyright holder. To view a copy of this licence, visit <http://creativecommons.org/licenses/by/4.0/>.

## Appendix A Machine Learning Methods

### A.1 Machine Learning preliminaries

As mentioned in the introduction, the recent renewed interest in the Z-minimisation problem has been motivated by its data-driven computational aspects related to the advent of large datasets of reflexive polytopes [11, 21]. Throughout this investigation, the intuition for several observations and main proofs was guided by the analysis of computational data of the 16 2-dimensional and 4319 3-dimensional reflexive polytopes used in [8]. In particular, neural networks and the gradient saliency method, similar to these in [22] were applied to judge which of the objects, including topological numbers of the resolution of the singularity and toric diagrams, are the most significant to the final result. We start by briefly introducing the relevant concepts.

#### A.1.1 Neural Networks

Neural Networks (NNs) are a class of supervised Machine Learning (ML) methods allowing approximation of highly non-linear maps of one or multiple variables we will call the *input* or *features*, to scalar or vector *outputs*. This is achieved by a series of processing layers applying subsequent operations to the original input and output of antecedent layers, by alternating linear and non-linear action such as the logistic sigmoid,

$$\sigma(x) = \frac{1}{1 + e^{-x}} \quad (\text{A1})$$

and ascribing 'weights' to the individual 'neurons'. The class of universal approximation theorems ensures that any continuous function can be approximated by an NN of sufficient number of layers or *depth*, or sufficient number of features, the *width* [23].

The usual avenue to discover the appropriate weights is to define a *loss function*  $L$  of both the input and the weights that measures how close the current outputs are to the true values and minimise it with respect to the weights.

#### A.1.2 The Gradient Saliency method

Neural Networks as such are often effectively black boxes - they do not provide any insight into inner workings of hidden layers by default. The term *saliency* refers to any effort to extract information about the inner workings of an ML model, NNs in particular. Here we use the method employed in [22], as aid in a study of knot theory notions which bears conceptual resemblance to our problem, called *gradient saliency*. It takes advantage of the fact that a loss function is a map of both the features and the weights. The principle is to examine how sensitive the loss function is to change in any given input variable, which provides intuition as to which of the features bear more on the final

result. Explicitly we calculate the (absolute values of) partial derivatives of the loss function with respect to features and average over the training set

$$s_i = \frac{1}{|\mathcal{F}|} \sum_{\mathbf{x} \in \mathcal{F}} \left| \frac{\partial L}{\partial \mathbf{x}_i} \right| \quad (\text{A2})$$

where the index  $i$  runs through the set of all features  $\mathcal{F}$  and  $\mathbf{x}$  refers to input examples. The relative sizes of  $s_i$ , provide the desired intuition. Furthermore, in our case multiple features are in fact vectors with up to 42 components. This could skew the proportions within the saliency analysis, so to remedy this the values of all components of such a feature were averaged, and the result included in the plot with a weight reciprocal to their number. All this is performed on the test set to avoid the influence of overfitting by some of the variables.

## A.2 Computational setup

A number of computational experiments were performed using the described tools and geometric data of the varieties in question. The starting point to all of them is the appropriate processing of the data in question. In our case of the 3-dimensional reflexive polytopes (in the 2-dimensional case the data was too scarce for deep learning attempts) the data included:

- the list of vertices of a polytope as coordinate tuples (fed into the network as flat row vectors padded with zeros where appropriate), referred to as *toric diagrams* for brevity,
- the first Chern number as well as the Euler number (which is proportional to the top Chern number) of the resolved singularity, collectively referred to as *topological numbers*,
- Euclidean volume of the polytope,
- the number of vertices and boundary points of the polytope collectively referred to as *point features*, and its polar dual (which allow to compute the Chern and Euler numbers of the full cone as observed in [8]),
- later the latter were also considered for polytopes scaled up from the original one by integer factors up to 6, similarly to the method in the pre-print <sup>1</sup>.

As in [22], the features were normalised to mean 0 and standard deviation 1, component-wise so across the vector features. The target output of the neural network was principally the normalised volume of  $Y$ , as shown in the example below. All these quantities, summarised in tab. A1 can be conveniently generated using `Sage`, save the critical Reeb vectors and associated volumes list available courtesy of Y-H. He.

Due to rather small size of the available full dataset the NN architecture was chosen not to be overly complex. This allowed easier extraction of relationships and computation time short enough to conveniently use it on a regular laptop.

---

<sup>1</sup>Berglund, P., Campbell, B., Jejjala, V.: Machine learning kreuzer-skarke calabi-yau threefolds (pre-print). arXiv:2112.09117 [hep-th] (2021)

After some prototyping it turned out that two hidden layers of logistic sigmoid of size 60 and 5 together with training in the batches of 60 over 1000 epochs were enough to produce satisfying accuracy. The matter of train-validation set split will be discussed in the subsequent section. All this was implemented using the Keras/Tensorflow package, as was the gradient saliency, and can be found in the GitHub repository<sup>2</sup>.

### A.3 Results and discussion

We now recount an example of a data experiment performed. The results shown below are all for the NN setup above, with 50-50 training-test split. Additionally, for these cases accuracy on both sets exhibited strong similarity, multiple splits were tested, with this tendency sustained each time. This phenomenon signifies that the NN is in fact learning the underlying mathematical structure, hence effective extrapolation to the test set, regardless of the portion of data seen [9, 16], and the pre-print<sup>3</sup>.

#### A.3.1 Learning the critical volumes

The initial motivation for usage of NNs was to assess whether there could be a procedure alternative to the tedious steps of Z-minimisation to find the critical volumes, which would be a valuable asset in tackling the problem in the Kreuzer-Skarke dataset. To this end, a regression problem to predict the critical volume was set up and trained with different sets of features shown in tab. A1.

Run	Choice of features
1	#vertices, #boundary points, $\text{vol}(\Delta)$ , $\Delta$ , $c_1(\tilde{X})$ , $\chi(\tilde{X})$
2	#vertices, #boundary points, $\text{vol}(\Delta)$ , $c_1(\tilde{X})$ , $\chi(\tilde{X})$
3	#vertices, #boundary points, $\text{vol}(\Delta)$ , $c_1(\tilde{X})$ , $\chi(\tilde{X})$ , $b^*$

**Table A1** Choice of features in subsequent runs of the experiment

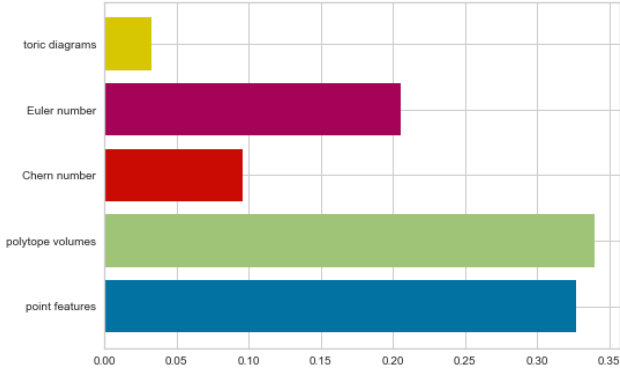
The network was able to predict the volumes with more than 80% accuracy, and exhibited the property that regardless of the train-validation split the accuracy was similarly high on all sets except for the run 1 containing the toric diagrams, as shown in tab. A2. This suggests that in most cases it indeed learned the mathematical structure of the problem rather than just overfit the training set, which clearly happened for run 1.

Gradient saliency analysis in the first run showed that by far the most important features were the number of vertices and boundary points, while the toric diagrams were in fact of marginal influence, as shown in fig. A1. Removing the toric diagrams from the list of features for run 2 confirmed

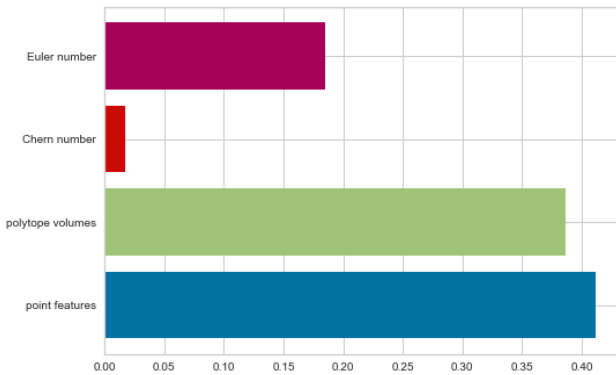
<sup>2</sup><https://github.com/lgrng/SasakiMLSaliency>

<sup>3</sup>Bao, J., He, Y.-H., Hirst, E., Hofscheier, J., Kasprzyk, A., Majumder, S.: Polytopes and machine learning (pre-print). arXiv:2109.09602 [hep-th] (2021)

Run	Training set accuracy (5%)	Training set accuracy (1%)	Test set accuracy (5%)	Test set accuracy (1%)
1	1.00000	0.99305	0.99770	0.84335
2	0.99814	0.81843	0.99885	0.79241
3	0.99861	0.86892	0.99885	0.83876

**Table A2** Critical volume learning experiment - summary of results**Fig. A1** Saliency analysis in run 1 of the experiment

this, as the test set accuracy remains similar and the training set accuracy drops to a comparable level prompting it indeed caused the overfitting. It is

**Fig. A2** Saliency analysis in run 2 of the experiment

understandable since the flattened and zero-padded vectors representing the diagram introduce multiple redundant parameters which are zero for most cases, as the number of vertices varies from 4 to 14.

So far, regardless of configuration the point features have remained significant for both runs. This could mean that the network is somehow able to produce a formula approximate to the original volume formula coming from the Hilbert series in eq. (41), together with its minimum. This appeared confirmed by

adding the critical Reeb vectors to the features list in run 3, which pushed the accuracy even higher, and was visible on the saliency plot in fig. A3.

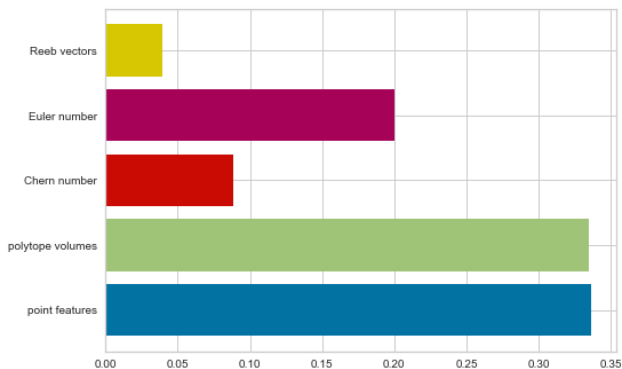


**Fig. A3** Saliency analysis in run 3 of the experiment

The possible conclusion is that the network is able to produce an approximate formula, akin to one describing the Euler number in the pre-print<sup>4</sup>, although we were not able to find its exact form. By the continuous approximation theorem, the original Z-minimisation procedure, being algorithmically obtainable from the toric diagram which is a finite set, should be visible to a sufficiently deep and wide network provided the dataset is large enough, for instance one working over a large sample of the Kreuzer-Skarke dataset, but in our case it was too shallow to be able to reproduce it.

## A.4 Summary

This investigation confirmed viability of machine learning as a helpful tool in tackling problems in geometry. In particular, the gradient saliency method successfully used in [22] proved to be equally effective here. While the heuristic ML methods are no "silver bullet" allowing to simplify any mathematical question whatever and all the results presented require significant amount of interpretation, they have the advantage of relatively easy implementation and scalability (we used similar architectures for various purposes with consistent effectiveness) comparing to the possible benefits. Indeed the most involved part of the procedure was data pre-processing which is inevitable for any data-reliant computational problem.

---

<sup>4</sup>Berglund, P., Campbell, B., Jejjala, V.: Machine learning kreuzer-skarke calabi-yau threefolds (pre-print). arXiv:2112.09117 [hep-th] (2021)

## References

- [1] Sparks, J.: Sasaki-einstein manifolds. *Surveys in Differential Geometry* **16**(1), 265–324 (2011). <https://doi.org/10.4310/sdg.2011.v16.n1.a6>
- [2] Martelli, D., Sparks, J.: Toric geometry, sasaki–einstein manifolds and a new infinite class of ads/cft duals. *Communications in Mathematical Physics* **262**(1) (2005). <https://doi.org/10.1007/s00220-005-1425-3>
- [3] Martelli, D., Sparks, J., Yau, S.-T.: Sasaki-einstein manifolds and volume minimisation. *Communications in Mathematical Physics* **280**(3), 611–673 (2008). <https://doi.org/10.1007/s00220-008-0479-4>
- [4] Martelli, D., Sparks, J., Yau, S.-T.: The geometric dual of a-maximisation for toric sasaki-einstein manifolds. *Communications in Mathematical Physics* **268**(1), 39–65 (2006). <https://doi.org/10.1007/s00220-006-0087-0>
- [5] Bergman, A., Herzog, C.P.: The volume of some non-spherical horizons and the ads/cft correspondence. *Journal of High Energy Physics* **2002**(01), 030–030 (2002). <https://doi.org/10.1088/1126-6708/2002/01/030>
- [6] Butti, A., Zaffaroni, A.: R-charges from toric diagrams and the equivalence of a-maximization and z-minimization. *Journal of High Energy Physics* **2005**(11), 019–019 (2005). <https://doi.org/10.1088/1126-6708/2005/11/019>
- [7] Futaki, A., Ono, H., Sano, Y.: Hilbert series and obstructions to asymptotic semistability. arXiv:0811.1315 [hep-th] (2010). Accessed 2022-09-14
- [8] He, Y.-H., Seong, R.-K., Yau, S.-T.: Calabi–yau volumes and reflexive polytopes. *Communications in Mathematical Physics* **361**(1), 155–204 (2018). <https://doi.org/10.1007/s00220-018-3128-6>
- [9] Krefl, D., Seong, R.-K.: Machine learning of calabi-yau volumes. *Physical Review D* **96**(6) (2017). <https://doi.org/10.1103/physrevd.96.066014>
- [10] Kreuzer, M., Skarke, H.: Reflexive polyhedra, weights and toric calabi-yau fibrations. *Reviews in Mathematical Physics* **14**(04), 343–374 (2002). <https://doi.org/10.1142/s0129055x0200120x>
- [11] Berman, D.S., He, Y.-H., Hirst, E.: Machine learning calabi-yau hypersurfaces. *Physical Review D* **105**(6), 066002 (2022). <https://doi.org/10.1103/PhysRevD.105.066002>
- [12] Boyer, C.P., Galicki, K.: *Sasakian Geometry*. Oxford Oxford Univ. Press,

Oxford (2008)

- [13] Silva, A.C.d.: Lectures on Symplectic Geometry. Springer, Berlin (2001)
- [14] Rukimbira, P.: Chern-hamilton's conjecture and k-contactness. *Houston Journal of Mathematics* **21** (1995)
- [15] Collins, T.C., Székelyhidi, G.: K-semistability for irregular sasakian manifolds. *Journal of Differential Geometry* **109**(1) (2018). <https://doi.org/10.4310/jdg/1525399217>
- [16] He, Y.-H.: The Calabi-Yau Landscape : from Geometry, to Physics, to Machine Learning. Springer, Cham, Switzerland (2021)
- [17] de Moraes, B. Suzana Falcão, Tomei, C.: Moment maps on symplectic cones. *Pacific Journal of Mathematics* **181**(2), 357–375 (1997)
- [18] Duistermaat, J., Heckman, G.: On the variation in the cohomology of the symplectic form of the reduced phase space. *Invent. math* **69**, 259–268 (1982)
- [19] Guillemin, V.: Kaehler structures on toric varieties. *Journal of Differential Geometry* **40**(2), 285–309 (1994). <https://doi.org/10.4310/jdg/1214455538>
- [20] Collins, T.C., Székelyhidi, G.: Sasaki-einstein metrics and k-stability. *Geometry and Topology* **23**(3), 1339–1413 (2019). <https://doi.org/10.2140/gt.2019.23.1339>
- [21] Bao, J., He, Y.-H., Hirst, E.: Neurons on amoebae. *Journal of Symbolic Computation* **116**, 1–38 (2023). <https://doi.org/10.1016/j.jsc.2022.08.021>
- [22] Davies, A., Veličković, P., Buesing, L., Blackwell, S., Zheng, D., Tomašev, N., Tanburn, R., Battaglia, P., Blundell, C., Juhász, A., Lackenby, M., Williamson, G., Hassabis, D., Kohli, P.: Advancing mathematics by guiding human intuition with ai. *Nature* **600**(7887), 70–74 (2021). <https://doi.org/10.1038/s41586-021-04086-x>
- [23] Goodfellow, I., Bengio, Y., Courville, A.: Deep Learning. MIT Press, Boston (2016). <http://www.deeplearningbook.org>